Methodological Comparison of Gravity-Driven and Matrigel-Embedded Fusion of Neurovascular-Immune Assembloids

Abstract

Human brain organoids model early neurodevelopment but lack vasculature and immunity, leading to hypoxic necrotic cores that limit maturation and translational relevance. Assembloid technology addresses this by fusing brain organoids with vascular-immune organoids (VIOs), yet no published study longitudinally compares fusion methods for brain–VIO pairs. This pilot establishes a standardised morphological tracking framework to evaluate scaffold-free gravity-mediated versus Matrigel-embedded fusion in size-matched organoid pairs (n = 5 per group). Longitudinal brightfield imaging across Days 2, 4, and 6 showed an apparent acceleration of morphological fusion in the gravity cohort, with 40% reaching complete consolidation by Day 6 versus 0% in the Matrigel cohort. However, an exact Mann–Whitney U test found no statistically significant difference at Day 6 ($p = 0.2778$), with interpretation limited by small sample size and high variability. Crucially, gravity-fused assembloids suffered catastrophic structural fracture during endpoint processing, whereas Matrigel-embedded assembloids remained intact and amenable to immunofluorescence. Confocal profiling of Matrigel assembloids at Day 7 revealed early CD31+ endothelial sprouting across the interface, but no detectable Iba1+ signal in the boundary zone. These findings define a practical engineering trade-off: gravity-mediated fusion may promote initial macroscopic contact but lacks the structural resilience required for standard histology under current conditions, while Matrigel embedding preserves tissue integrity and enables cellular readouts despite slower apparent fusion. The study identifies key bottlenecks - processing survivability, timeline for immune integration, and detection limits - and outlines next steps including extended culture, chemokine supplementation, and improved imaging. This work provides a technical baseline for building robust, vascularised brain models for neurovascular and neuroinflammatory disease research.

Keywords: organoid assembloid; brain organoid; vascular immune organoid; fusion kinetics; immunofluorescence staining; tissue engineering

1. Introduction

1.1 Limitations of Standalone Brain Organoid Culture

Human brain organoids (BO) are self-assembling three-dimensional in vitro models that recapitulate key architectural and developmental features of the early human central nervous system. Despite their utility for investigating neurogenesis, cortical patterning, and neurological disease phenotypes, these models

suffer from a well-characterised critical flaw: an absence of endogenous vascular and immune tissue compartments. Without perfusable microvessels, oxygen, nutrients, and soluble signalling factors can only diffuse approximately 200 μm into organoid tissue from the external media boundary. This limited diffusion gradient drives the formation of a hypoxic, metabolically deprived necrotic core within larger organoid masses, suppressing neural progenitor proliferation, impairing neuronal functional maturation, and drastically reducing translational relevance for modelling neurovascular and neuroinflammatory pathologies. Hypoxia-induced central necrosis remains the primary technical bottleneck restricting long-term BO culture complexity.

1.2 Assembloids as a Neurovascular Unit Modelling Platform

Assembloid technology circumvents the avascular limitation of pure BOs through heterotypic fusion of distinct organoid subtypes to enable direct tissue–tissue paracrine signalling and structural integration. Co-culturing BOs with vascular immune organoids (VIOs) enables reconstruction of an in vitro neurovascular unit containing neural tissue, endothelial vascular networks, perivascular support cells, and resident microglial immune populations. Unlike tissue sources limited to pure endothelium, VIOs concurrently generate both vascular and innate immune lineages within a single self-organised construct, removing the need for multiple independent mesodermal tissue sources to reconstitute brain vasculature and immunity in parallel. Published in vitro data demonstrate that vascularised assembloids mitigate central hypoxia, reduce spontaneous necrotic cell death, expand proliferative neural progenitor pools, and yield neuronal subpopulations with enhanced electrophysiological maturation relative to avascular BO monocultures.

1.3 Unresolved Gap in Fusion Protocol Characterisation

Two distinct culture methodologies are routinely employed to facilitate organoid fusion for assembloid generation, yet no published quantitative longitudinal comparison evaluates their performance specifically for BO-VIO pairs.

1. Scaffold-free gravity-mediated fusion: Organoids sediment into direct contact at the conical base of ultra-low attachment (ULA) U-bottom 96-well plates; tissue merging proceeds exclusively via spontaneous homotypic and heterotypic cell–cell adhesion without exogenous extracellular matrix support.
2. Matrigel dome embedding fusion: Matched organoid pairs are co-encapsulated within a polymerised hydrogel droplet, providing mechanical confinement, basement membrane

laminin/collagen substrates, and soluble growth factor cues to accelerate cell migration and tissue attachment across the organoid interface.

Critical engineering trade-offs remain uncharacterized for this co-culture system. It remains unknown whether Matrigel embedding provides the structural reinforcement necessary to withstand downstream laboratory processing, or if scaffold-free gravity aggregation can achieve comparable morphological integration over extended culture without matrix shielding. Furthermore, the lack of longitudinal kinetic profiling across early culture timepoints introduces severe baseline variability into downstream neurovascular and neuroinflammatory modelling protocols within our laboratory. This pilot study addresses this technical gap by establishing a standardised morphological tracking framework.

2. Materials and Methods

2.1 Organoid Source and Pre-Experimental Standardisation

Developmentally synchronised BOs and VIOs were generated via established laboratory differentiation protocols prior to fusion setup. All organoids were size-sorted under brightfield microscopy to isolate uniform diameter constructs for pairing, eliminating size-dependent fusion variability as a confounding variable.

2.2 Fusion Culture Setup

Two experimental fusion groups were established in parallel under identical incubator conditions (37 °C, 5% CO_2, humidified atmosphere), with five assembloids per group (n = 5):

1. Matrigel embedding fusion: Cold growth-factor-reduced Matrigel was dispensed as uniform domes into 6-well tissue culture plates; one BO and one VIO were placed within each liquid hydrogel droplet. Plates were incubated at 37 °C for 30 min to permit full Matrigel polymerisation, after which equal volumes of complete organoid culture media were overlaid atop each dome.
2. Gravity-mediated scaffold-free fusion: Low volumes of pre-warmed complete media were added to U-bottom ultra-low attachment 96-well plates; one BO and one VIO were seeded into each well, allowing passive sedimentation into central tissue contact without ECM supplementation.

All experimental wells received consistent half-media changes at 48-hour intervals throughout the 7-day culture period to eliminate differential nutrient or oxygen limitation between groups.

2.3 Longitudinal Brightfield Imaging

Whole-well brightfield micrographs of all fused assembloids were acquired at three discrete culture timepoints: Day 2, 4, 6 post-fusion assembly. Fixed microscope lamp intensity, exposure time, condenser aperture, and objective magnification parameters were maintained across all imaging sessions to standardise downstream segmentation analysis.

2.4 Immunofluorescence Staining

Following the culture period, assembloids were harvested for histological validation. To map the internal cell architecture and cellular intermingling across the fusion boundary, a four-channel fluorescent marker panel was applied. Slides were stained using DAPI (to visualise all cell nuclei), Pax6 (to identify cortical neural progenitor cells/radial glia within the host BO), CD31 (to identify endothelial blood vessels sprouting from the VIO), and Iba1 (targeting macrophages to assess immune integration).

While Matrigel-embedded samples remained macroscopically intact during harvesting and matrix depolymerisation, scaffold-free gravity-mediated assemblies experienced catastrophic structural fracture at the fusion interface during processing. Consequently, downstream immunofluorescence imaging was successfully completed for the matrix-embedded cohort only (n = 1), though the potential for chemical depolymerisation to induce minor localised microstructural artefacts in the embedded cohort cannot be ruled out.

2.5 Image Quantification

2.5.1 Brightfield Micrographs

Rather than using automated pixel tracking or digital image pre-processing, a standardised ordinal ranking system was used to score the visual morphological consolidation of each assembloid pair. Samples were examined manually and assigned a score based on the physical appearance of the contact interface.

- Rank 0 (No Fusion): Two distinct spheres merely touching; sharp 180° clefts visible at the interface.
- Rank 1 (Partial Fusion): Physical tissue bridge formed; contact clefts visibly flatten, but individual organoid spheres remain clearly identifiable.
- Rank 2 (Complete Fusion): Tissues fully integrated into a single continuous elongated or spherical mass; the interface boundary line is completely absent.

2.5.2 Immunofluorescence Staining

To evaluate cellular integration across the neurovascular boundary, confocal microscopy images of the Matrigel-embedded group were analysed qualitatively on Day 7 post-fusion. Image analysis focused on verifying the presence and distribution of CD31+ endothelial structures and macrophages across the interface zone, assessing whether these migrating populations successfully crossed the superficial boundary layer to intermingle with the host BO tissue.

2.6 Statistical Analysis

Statistical analysis was performed to compare the ordinal fusion scores between the Matrigel-embedded and scaffold-free gravity-mediated groups. Because the fusion kinetics were evaluated using a non-continuous, ordinal ranking system (scores 0–2), non-parametric testing was required. A cross-sectional Mann-Whitney U test was used to determine whether there were statistically significant differences in the physical fusion scores between the two experimental methods at the final Day 6 endpoint.

3. Results

3.1 Longitudinal Brightfield Tracking

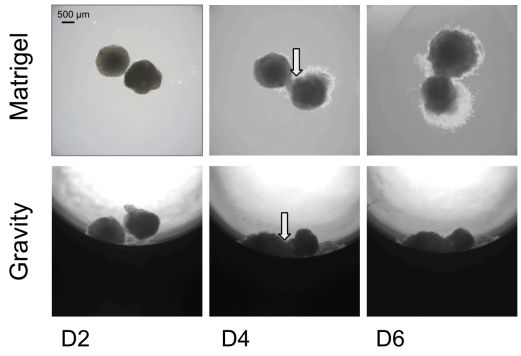

Figure 1. Representative brightfield images of assembloids. White arrows indicate initial tissue contact zones at Day 4.

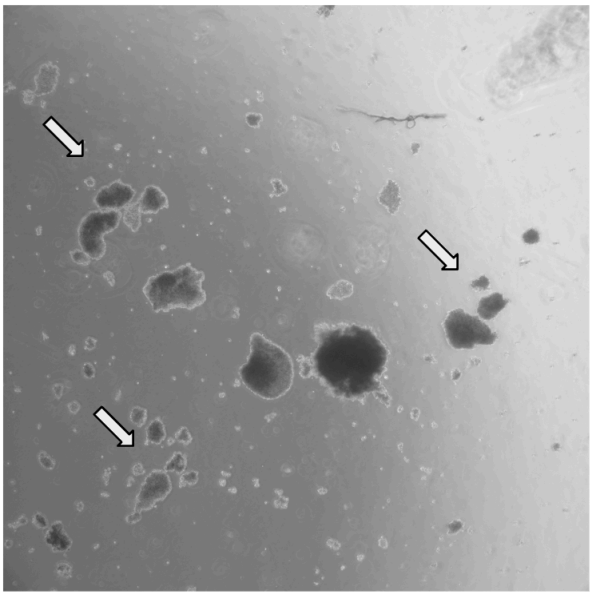

Figure 2. Interfacial dissociation and structural vulnerability in scaffold-free cultures. Representative brightfield micrograph capturing macro-structural failure during endpoint chemical processing.

Longitudinal brightfield tracking revealed distinct macrostructural trajectories between the two fusion protocols over the 7-day culture period. In the early post-fusion phase (Days 2, 4), scaffold-free gravity-mediated assemblies exhibited rapid physical contact and macroscopic alignment, driven by passive sedimentation at the conical base of the ultra-low-attachment wells (**Figure 1**). However, this initial proximity did not translate into superior long-term tissue consolidation. Fragmentation was observed in the gravity group during endpoint processing; routine media exchange and handling are plausible contributors, but the specific mechanism was not directly tested. (**Figure 2**). This structural decay led to severe tissue fragmentation and complete mechanical failure during harvesting and subsequent downstream manipulation. Conversely, while Matrigel-embedded assembloids exhibited less immediate initial macroscopic contact, the polymerised hydrogel droplet served as a critical external basement membrane scaffold (**Figure 1**).

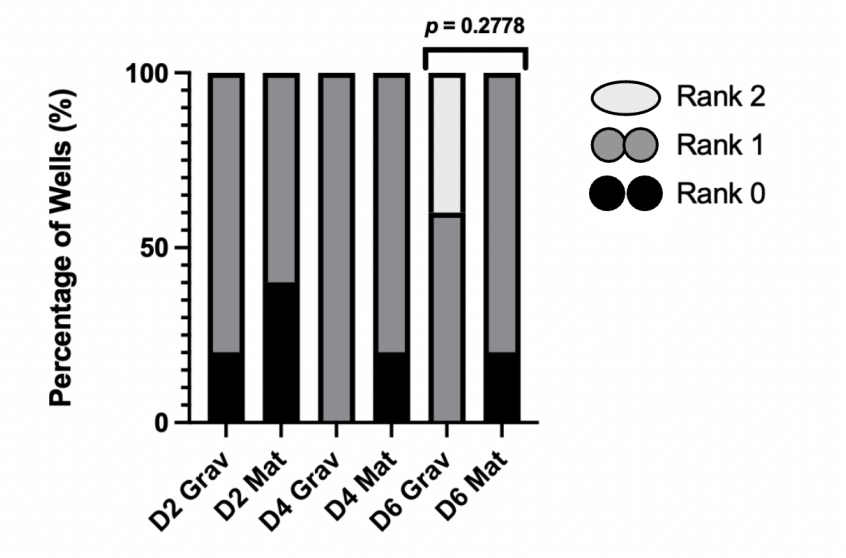

Figure 3. Assembloid fusion kinetics. Longitudinal distribution of morphological fusion ranks across Days 2, 4, and 6 (n = 5 per group). Rank 0: Unfused spheres. Rank 1: Partial dumbbell bridge. Rank 2: Complete consolidated mass. Statistical variance at Day 6 was evaluated via an unpaired, non-parametric Mann-Whitney U test (p = 0.2778).

Longitudinal profiling in Figure 3 showed an apparent acceleration of morphological fusion in the scaffold-free gravity cohort compared with the Matrigel-embedded group across all timepoints. By Day 2, fewer gravity assemblies remained unfused (Rank 0: 20%) than Matrigel assemblies (40%). By Day 4, all gravity-driven assemblies had reached at least partial fusion (Rank 1: 100%), whereas 20% of Matrigel domes remained completely unfused (Rank 0). At Day 6, only the gravity cohort achieved complete consolidation (Rank 2: 40%), while the Matrigel cohort yielded no Rank 2 assemblies (0%) and still had 20% at Rank 0. However, a cross-sectional Mann-Whitney U test performed on the Day 6 ordinal scores indicated that this morphological advantage was not statistically significant ($p = 0.2778$), with interpretation limited by the small sample size ($n = 5$ per group) and high variability between organoid pairs. These findings therefore represent an exploratory morphological trend rather than statistically confirmed evidence of faster fusion for the gravity-assisted method.

3.2 Confocal Characterisation of Cellular Integration

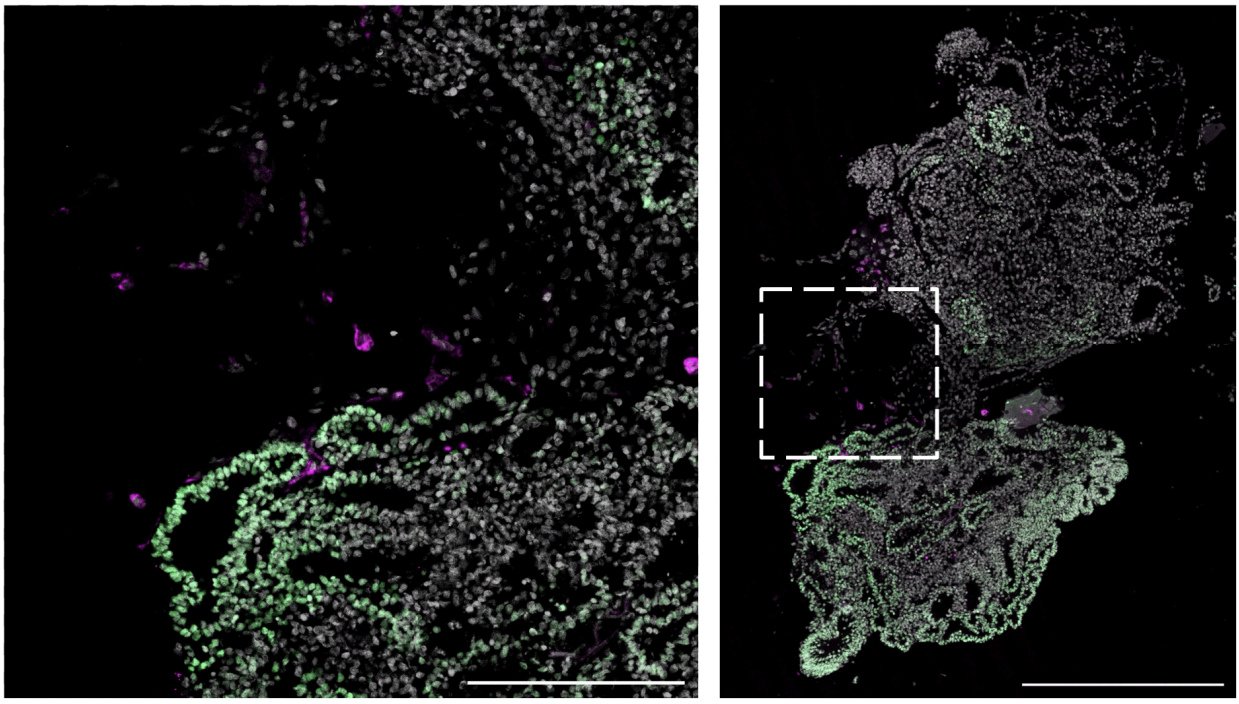

Figure 4. Confocal immunofluorescence characterisation of cellular integration across the matrix-embedded neurovascular interface at Day 7 post-fusion. Representative tile-scan confocal image (right; scale bar = 500 µm) showing the spatial arrangement of the macro-structural interface between BO and VIO co-encapsulated within a Matrigel dome scaffold. The dashed white bounding box denotes the high-magnification region of interest (left; scale bar = 200 µm) focusing on the localised tissue boundary. Multi-channel fluorescence profiles highlight cell nuclear distribution (grey), distinct cortical neural progenitors lining the outer borders (green), and localised microvascular structural morphology sprouting across the superficial boundary line (magenta). While the four-channel panel included Iba1 (blue) targeting macrophages, distinct Iba1+ immunofluorescent signals were completely absent across the tracked interface zone at this timepoint.

To evaluate cellular intermingling across the consolidated neurovascular boundary, confocal immunofluorescence analysis was performed on Day 7 post-fusion. Due to the systematic structural fracture and fragmentation of the scaffold-free gravity cohort during processing, downstream histological and immunofluorescence imaging was successfully completed for the matrix-embedded cohort only.

Four-channel fluorescent marker profiling of the surviving Matrigel-embedded assembloids verified early-stage, localised neurovascular integration (**Figure 4**). Endothelial structures sprouting from the VIO successfully crossed the superficial interface boundary, with distinct (CD31) blood vessels actively infiltrating the outer cortical layers of the (Pax6) host BO tissue. In contrast to this rapid angiogenic sprouting, analysis of the innate immune compartment revealed an absence of distinct (Iba1) macrophage signals migrating across the interface zone. While the external matrix successfully preserved the structural

macro-architecture necessary for spatial integration, multi-lineage cellular infiltration remained incomplete at this baseline endpoint.

4. Discussion

The experimental findings reveal a complex tissue engineering trade-off between immediate interfacial proximity and long-term macrostructural survivability. Under brightfield microscopy, the scaffold-free gravity method exhibits tighter macroscopic contact and alignment in early culture phases, likely because gravitational force directly compresses the spheres together. However, this physical proximity did not translate into functional structural integration during downstream histological processing. Beyond the baseline absence of an external matrix framework, this localised interface fragmentation may be further compounded by discrete biochemical and physical factors. Biochemically, the specialised culture media composition may lack optimal calcium concentrations or specific trophic factors required to strongly upregulate homotypic and heterotypic cadherin binding at a bare cell-to-cell interface. Physically, without a protective hydrogel shield, the unreinforced, naked tissue bridge is completely exposed to fluid dynamic shear stress. The accumulated mechanical force generated during routine manual pipetting for 48-hour half-media changes likely introduced micro-fractures along the fragile interface boundary line, ultimately driving complete tissue collapse during harvesting.

Conversely, the Matrigel-embedded protocol provides the necessary structural reinforcement to preserve tissue viability during routine laboratory manipulation, even though initial macroscopic contact appears less immediate. At Day 7 post-fusion, this matrix support successfully maintained tissue integrity and facilitated early-stage, localised integration, as evidenced by (CD31+) blood vessels infiltrating the superficial layer of the BO. However, this integration was strictly non-uniform and lacked any detectable macrophage infiltration across the boundary. The absence of detectable Iba1-positive cells at the interface may reflect several factors. First, 7 days post-fusion may be insufficient for myeloid cells to mature, expand, and migrate across the boundary, especially in the absence of chemokine cues such as CX3CL1. Second, Iba1 expression in this vascular–immune organoid system may be low or heterogeneous at this stage, limiting detection. Third, macrophage-like cells may be present but confined to regions outside the imaged field or at depths not captured in this tile scan. Finally, technical factors such as antibody penetration, fixation conditions, or signal attenuation in thick organoid tissue could reduce sensitivity. Distinguishing between true biological non-migration and technical non-detection will require later timepoints, broader sampling, and validation of Iba1 staining in the VIO monoculture.

Several key methodological limitations influenced the outcomes of this pilot study and must be addressed in future work. A fundamental conceptual limitation of this study's tracking framework is the conflation of passive morphological flattening with genuine biological parenchymal fusion within the ordinal ranking criteria. While the manual scoring system registered an advanced fusion phenotype (Rank 2) for the gravity cohort by Day 6 based on outline consolidation, a 2D top-down optical projection cannot differentiate between active cellular intermingling and passive gravitational settling or superficial cellular spreading against the ultra-low attachment well surface. The catastrophic structural fracture of the gravity assemblies during endpoint harvesting strongly suggests that the observed consolidation was mechanical flattening rather than functional tissue integration. Because this mechanical failure precluded downstream immunofluorescence validation, the true internal cellular integration state of the scaffold-free cohort remains entirely unverified, making the biological significance of the apparent kinetic advantage uncertain. Furthermore, evaluating the assembloids at Day 7 post-fusion represents an insufficient timeline for multi-lineage integration. While 7 days was long enough to capture early-stage, superficial angiogenic sprouting (CD31+) infiltration, it proved insufficient for slower-moving, unprimed innate immune populations (Iba1+ macrophages) to mature, expand, or actively migrate across the neurovascular interface.

To address the constraints identified in this study, future research should focus on optimising the post-fusion timeline, biochemical environment, and fluidic handling protocols. Extending the culture window past Day 14 is an essential next step to determine if longer incubation allows slower-moving macrophage populations to successfully migrate into host brain tissue, an effort that could be actively accelerated by incorporating localised chemokine gradients such as CX3CL1 to recruit immune cells across the boundary. Biochemically, adjusting the composition of specialised media – specifically via calcium supplementation – could enhance cadherin binding stability. Alternatively, testing a hybrid matrix approach, such as a temporary, lower-density or synthetic shear-thinning hydrogel, could help strike an optimal balance between initial physical stability and uninhibited cellular migration.

In conclusion, this pilot study highlights that engineering complex neurovascular assembloids relies heavily on a multi-factorial trade-off between physical tissue support and cellular migration kinetics. Our findings demonstrate that while scaffold-free gravity methods may promote rapid initial tissue contact, they lack the macrostructural resilience required to survive standard laboratory processing, resulting in tissue fragmentation. On the other hand, Matrigel embedding provides the structural viability necessary for successful downstream imaging, revealing early-stage, superficial blood vessel infiltration (CD31+) by Day 7 post-fusion. While multi-lineage integration could not be confirmed at this early timepoint, as Iba1-positive cells were not detected in the imaged interface region, this project establishes a valuable

technical baseline for structural handling, moving us one step closer to building reliable, vascularized brain models for disease research.

Acknowledgements

This research was supported by the Laidlaw Undergraduate Scholars Programme. The author thanks laboratory supervisors for experimental guidance, technical staff for organoid culture maintenance support, and peers for critical feedback on imaging quantification pipelines.